Purcell factor for a point-like dipolar emitter coupled to a two-dimensional plasmonic waveguide

J. Barthes, G. Colas des Francs,[*] A. Bouhelier, J.-C. Weeber, and A. Dereux

Laboratoire Interdisciplinaire Carnot de Bourgogne, UMR 5209 CNRS – Université de Bourgogne, 9 Avenue A. Savary,
BP 47 870, F-21078 Dijon, France

We theoretically investigate the spontaneous emission of a point-like dipolar emitter located near a two-dimensional plasmonic waveguide of arbitrary form. We invoke an explicit link with the density of modes of the waveguide describing the electromagnetic channels into which the emitter can couple. We obtain a closed form expression for the coupling to propagative plasmon, extending thus the Purcell factor to plasmonic configurations. Radiative and nonradiative contributions to the spontaneous emission are also discussed in detail.

In 1946, Purcell demonstrated that spontaneous emission of a quantum emitter is modified when located inside a cavity.[1] A critical parameter is the ratio $Q/V_{\rm eff}$, where Q and $V_{\rm eff}$ refer to the cavity mode quality factor and effective volume, respectively. In the weak-coupling regime, the Purcell factor F_p quantifies the emission rate γ inside the cavity compared to its free-space value γ_0

$$F_p = \frac{\gamma}{n_1 \gamma_0} = \frac{3}{4\pi^2}\left(\frac{\lambda}{n_1}\right)^3 \frac{Q}{V_{\rm eff}}, \qquad (1)$$

where λ is the emission wavelength and n_1 the cavity optical index. When $Q/V_{\rm eff}$ is high enough, a strong-coupling regime occurs with reversible energy exchange between the emitter and the cavity mode (Rabi oscillations).[2] The design of cavities maximizing this ratio in order to control spontaneous emission is extremely challenging. There is however a trade off between Q factor and effective volume. On one side, ultrahigh Q ($\sim 10^9$) are obtained in microcavities but with large effective volume ($\sim 10^3$ μm^3). On the other side, diffraction-limited mode volumes [$V_{\rm eff} \sim (\lambda/n_1)^3$] are achieved in photonic crystals but at the price of weaker quality factors ($Q \sim 10^5$). Moreover, it is sometimes preferable to optimize $Q/V_{\rm eff}$ but keeping a reasonable Q factor in order to efficiently extract the signal from the cavity. Additionally, the emitter spectrum can be large at ambient temperature, and better coupling is expected with low-Q cavities[3] (i.e., matching cavity and emitter impedances[4]).

In this context, it has been proposed to replace the cavity (polariton) mode by a surface plasmon polariton (SPP) sustained by metallic structures as an alternative to cavity quantum electrodynamics.[5,6] SPP can have extremely reduced effective volume, ensuring high coupling rate with quantum emitters, albeit a poor quality factor [$Q \sim 100$ (Ref. 7)]. Particularly, coupling an emitter to a plasmonic wire sheds new light on manipulating a single photon source at a strongly subwavelength scale, with applications for quantum information processing.[8] Others promising applications deal with the realization of integrated plasmonic amplifiers.[9–11] Highly resolved surface spectroscopy was also pointed out based either on the antenna effect[12] or coupling dipolar emission to an optical fiber via a plasmonic structure.[13,14]

In this work, we present an original approach for calculating rigorously the coupling of a dipolar emitter to two-dimensional

(2D) plasmonic waveguides of arbitrary profile. We achieve a closed-form expression for the coupling rate into the guided SPP. We also investigate the radiative and nonradiative channels. In particular, the contribution of the plasmon, difficult to estimate otherwise,[5,15] is clearly established. Our method is general and treats equivalently bound and leaky waveguides of arbitrary cross section, possibly on a substrate (Fig. 1).

According to Fermi's golden rule, coupling of a quantum emitter to a continuum of modes is governed by the (3D) local density of states (3D-LDOS):

$$\gamma(\mathbf{r}) = \frac{2\pi\omega}{\hbar\epsilon_0}|p|^2 \rho_{\mathbf{u}}(\mathbf{r},\omega), \qquad (2)$$

where $\rho_{\mathbf{u}}(\mathbf{r},\omega)$ is the local density of modes, projected along the direction of the dipolar transition moment $\mathbf{p} = p\mathbf{u}$ (partial LDOS).[16] $\mathbf{r}$ is the emitter location and ω its emission frequency. To characterize the coupling independently of the emitter properties, we introduce the normalized quantity $\gamma(\mathbf{r})/\gamma_0 = \rho_{\mathbf{u}}(\mathbf{r},\omega)/\rho_{\mathbf{u}}^0(\omega)$, where $\rho_{\mathbf{u}}^0(\omega) = \omega^2/6\pi^2 c^3$ is the free-space partial LDOS.

Since we are interested in 2D waveguides, the main idea is to work on the density of modes associated with the guide (bound and radiation modes). For this purpose, we now establish a relationship between 2D and 3D LDOS by introducing Green's dyad formalism. First, the 3D-LDOS is related to
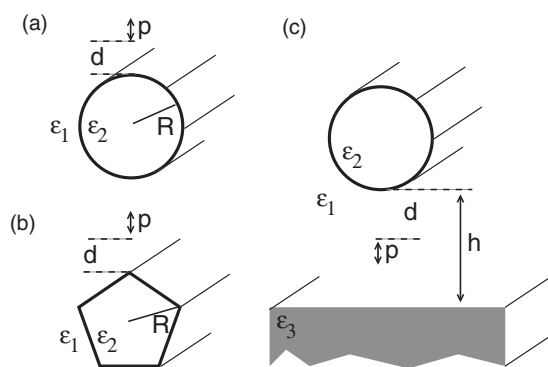

FIG. 1. Practice models. A dipolar emitter **p** is located at distance d of an infinite silver cylinder of circular (a) or pentagonal (b) cross section. (c) The dipolar emitter is located in a substrate-wire gap.

the 3D Green's tensor **G** of the system (Im and Tr refer to the imaginary part and trace):[17]

$$\rho(\mathbf{r}) = -\frac{k_0^2}{\pi\omega}\,\mathrm{Im}\,\mathrm{Tr}\,\mathbf{G}(\mathbf{r},\mathbf{r})\,. \quad (3)$$

In the presence of an infinitely long (2D) structure, the 3D-Green's tensor is expressed by a Fourier transform:

$$\mathbf{G}(\mathbf{r},\mathbf{r}') = \frac{1}{2\pi}\int_{-\infty}^{\infty}dk_z\,\mathbf{G}^{2D}(\mathbf{r}_\parallel,\mathbf{r}_\parallel',k_z)e^{-ik_z(z-z')}\,. \quad (4)$$

Then, we obtain the 3D-LDOS as a function of 2D-Green's dyad:

$$\rho(\mathbf{r}) = -\frac{k_0^2}{2\pi^2\omega}\int_{-\infty}^{\infty}dk_z\,\mathrm{Im}\,\mathrm{Tr}\,\mathbf{G}^{2D}(\mathbf{r}_\parallel,\mathbf{r}_\parallel,k_z)\,. \quad (5)$$

Equation (5) obviously reproduces the 3D-LDOS in a homogeneous medium of index n_1. Limiting the integration range to radiative waves, and since $-\frac{k_0^2}{\pi\omega}\,\mathrm{Im}\,\mathrm{Tr}\,\mathbf{G}_{\mathrm{hom}}^{2D}(\mathbf{r}_\parallel,\mathbf{r}_\parallel,k_z) = \omega/2\pi c^2$ in a homogeneous medium, we obtain, as expected, $\rho_0(\mathbf{r}) = \frac{1}{2\pi}\int_{-n_1k_0}^{n_1k_0}dk_z\,\omega/2\pi c^2 = n_1\omega^2/2\pi^2c^3$. The quantity $-\frac{k_0^2}{\pi\omega}\,\mathrm{Im}\,\mathrm{Tr}\,\mathbf{G}^{2D}(\mathbf{r}_\parallel,\mathbf{r}_\parallel,k_z)$ is generally referred as 2D-LDOS by analogy with 3D-LDOS expression (3).[18] It is a key quantity to understand spatially and spectrally resolved electron energy loss spectroscopy.[19] Equation (5) makes then a direct link between 2D and 3D LDOS. We however consider a slightly different definition, more appropriate to describe a density of guided modes:[20]

$$\rho^{2D}(\mathbf{r}_\parallel,k_z) = -\frac{2k_z}{\pi}\,\mathrm{Im}\,\mathrm{Tr}\,\epsilon(\mathbf{r}_\parallel)\mathbf{G}^{2D}(\mathbf{r}_\parallel,\mathbf{r}_\parallel,k_z)\,. \quad (6)$$

The 2D Green's dyad is separated in two contributions $\mathbf{G}^{2D} = \mathbf{G}_{\mathrm{ref}}^{2D} + \Delta\mathbf{G}^{2D}$ where $\mathbf{G}_{\mathrm{ref}}^{2D}$ is the 2D-Green's dyad without the waveguide and $\Delta\mathbf{G}^{2D}$ is the guide contribution. This formulation separates the reference system (multilayer substrate, homogeneous background, . . .) from the guiding structure. It comes with ϵ_{ref} the dielectric constant of the reference system,

$$\rho^{2D}(\mathbf{r}_\parallel,k_z) = \rho_{\mathrm{ref}}^{2D}(\mathbf{r}_\parallel,k_z) + \Delta\rho^{2D}(\mathbf{r}_\parallel,k_z), \quad \text{with}$$

$$\rho_{\mathrm{ref}}^{2D} = -\frac{2k_z}{\pi}\,\mathrm{Im}\,\mathrm{Tr}\,\epsilon_{\mathrm{ref}}(\mathbf{r}_\parallel)\mathbf{G}_{\mathrm{ref}}^{2D}(\mathbf{r}_\parallel,\mathbf{r}_\parallel,k_z), \quad (7)$$

$$\Delta\rho^{2D} = -\frac{2k_z}{\pi}\,\mathrm{Im}\,\mathrm{Tr}\,\epsilon(\mathbf{r}_\parallel)\Delta\mathbf{G}^{2D}(\mathbf{r}_\parallel,\mathbf{r}_\parallel,k_z)\,.$$

This wording separates the continuum of modes of the reference system ρ_{ref}^{2D} from the waveguide density of modes $\Delta\rho^{2D}$. The partial 2D-LDOS is finally

$$\Delta\rho_{\mathbf{u}}^{2D}(\mathbf{r}_\parallel,k_z) = -\frac{2k_z}{\pi}\,\mathrm{Im}\,\mathrm{Tr}\,\epsilon(\mathbf{r}_\parallel)[\mathbf{u}\cdot\Delta\mathbf{G}^{2D}(\mathbf{r}_\parallel,\mathbf{r}_\parallel,k_z)\cdot\mathbf{u}]\,. \quad (8)$$

Figure 2 represents the radial 2D-LDOS $\Delta\rho_r^{2D}(k_z)$ for the benchmark model defined in Fig. 1(a). The 2D Green's dyad has been numerically evaluated by applying a meshing on the waveguide cross section.[20] The main contribution is the Lorentzian variation peaked at the effective index of the guided SPP $n_{\mathrm{eff}} = k_{\mathrm{SPP}}/k_0 = 2.28$, and with a full width at half maximum inversely proportional to the mode propagation length
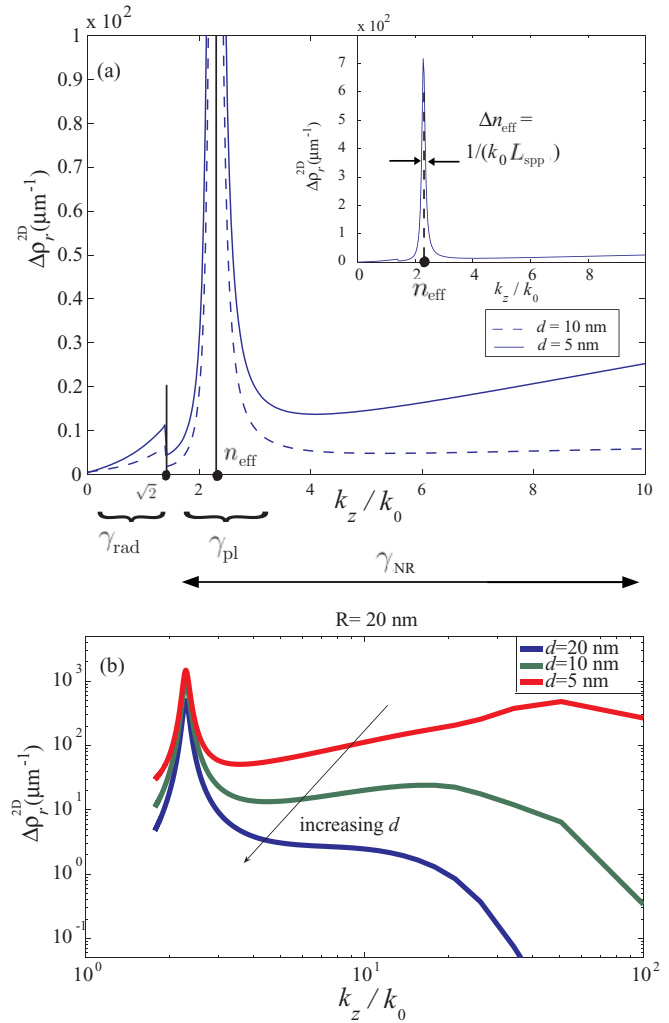

FIG. 2. (Color online) (a) 2D radial LDOS variation as a function of k_z at two distances to the nanowire of Fig. 1(a). (b) Log scale over the high momentum range. $R = 20$ nm, $\epsilon_2 = -50 + 3.85i$, $\lambda = 1$ μm, and $\epsilon_1 = 2$.

$L_{\mathrm{spp}} = 1.2$ μm (inset). For $k_z < n_1k_0$, the 2D-LDOS describes scattering events and contributes to radiative rate γ_{rad}. Finally, for $k_z > n_1k_0$, LDOS takes part in the nonradiative decay rate γ_{NR}. Indeed, the plasmon is dissipated by thermal losses. Moreover, for very short distances, the 2D-LDOS spectrum extends over very large values of k_z [Fig. 2(b)]. This behavior is typical for nonradiative transfer by electron-hole pair creation in the metal.[21]

The coupling rate into the propagative SPP is obtained using Eqs. (3), (5), and (8) and keeping only the plasmon contribution by limiting the integration of Eq. (5) to k_z corresponding to the SPP resonance. This is strongly simplified by the Lorentzian shape of the resonance and leads to the closed-form expression[11]

$$\frac{\gamma_{\mathrm{pl}}}{n_1\gamma_0} = \frac{3\pi\lambda}{4n_1^3k_{\mathrm{SPP}}}\frac{\Delta\rho_{\mathbf{u}}^{2D}(\mathbf{r}_\parallel,k_{\mathrm{SPP}})}{L_{\mathrm{spp}}}\,. \quad (9)$$

This important result describes the emitter coupling rate to a 2D waveguide of arbitrary cross section. It is expressed as the overlap between the dipolar emission and the guided
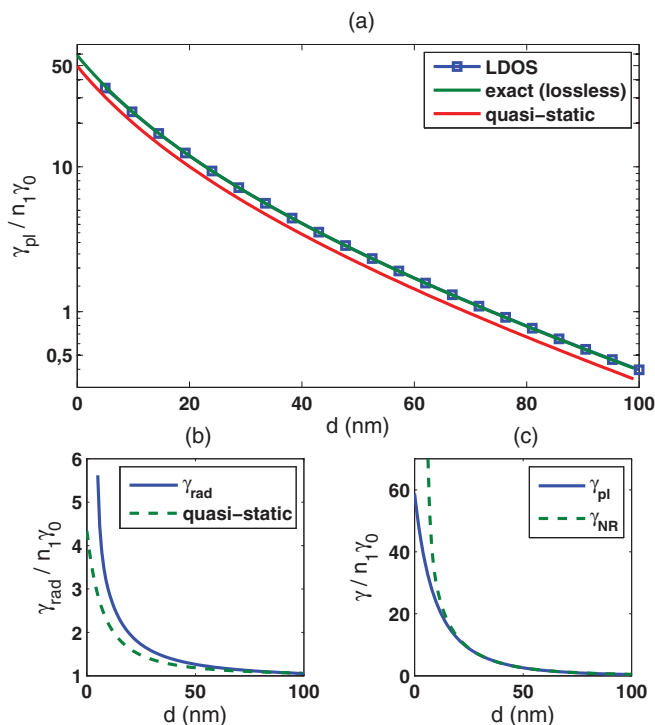
FIG. 3. (Color online) Variation of the rates as a function of distance to the silver nanowire for a radial dipole. (a) Coupling rate into SPP obtained using (i) our approach based on 2D-LDOS formulation, *including losses*, (ii) exact *lossless* case, and (iii) quasistatic approximation. (b) Radiation rate calculated using 2D-LDOS formulation (solid line) or quasistatic approximation (dotted line). (c) Comparison of the plasmon rate γ_{pl} with the total nonradiative rate γ_{NR}.
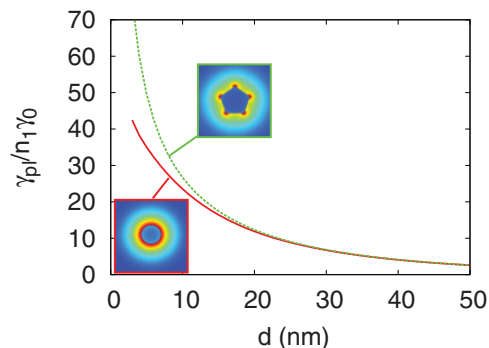

FIG. 4. (Color online) Coupling rate to guided SPP calculated near a cylindrical wire of circular (solid red/gray line) or pentagonal (dotted green/light gray line) cross section ($R = 20$ nm). The mode profiles are shown.

mode profile ($\Delta\rho_{\mathbf{u}}^{2D}$) divided by the mode propagation length in the longitudinal direction. This defines the 3D Purcell factor for a 2D geometry. Although presented for plasmonic waveguide, the demonstration remains valid for any 2D configuration (plasmonic cavity[7] or waveguide,[11] metal-coated[3] or dielectric[22] nanofiber, . . .). In order to validate this expression, we now compare it to the exact expression obtained by considering coupling to a *lossless* waveguide:[22,23]

$$\frac{\gamma_{pl}}{\gamma_0} = \frac{3\pi c E_{\mathbf{u}}(d)[E_{\mathbf{u}}(d)]^*}{k_0^2 \int_{A_\infty} (\mathbf{E} \times \mathbf{H}^*) \cdot \mathbf{z}\, dA}, \qquad (10)$$

where ($\mathbf{E},\mathbf{H}$) is the electromagnetic field associated with the guided SPP. In Fig. 3(a), we compare the coupling rate into the plasmonic channel as a function of distance to the silver nanowire obtained using (i) closed-form expression (9), (ii) exact expression for a *lossless* plasmonic waveguide (10), and (iii) a quasistatic approximation.[5]

Quite surprisingly, although the exact expression neglects dissipation, we obtain an excellent agreement with our expression that correctly accounts for losses. In formula (9) the ratio $\Delta\rho_{\mathbf{u}}^{2D}/L_{spp}$ is proportional to the number of guided modes[20] so that it does not depend on the losses. When losses tend toward zero, $L_{SPP} \to \infty$ and $\Delta\rho_{\mathbf{u}}^{2D} \to \infty$ at resonance so that $\Delta\rho_{\mathbf{u}}^{2D}/L_{spp}$ remains constant (Dirac distribution). Equivalently, this simply reveals that the emitter couples to

the guided mode, no matter whether the energy is dissipated by losses during propagation or propagates to infinity.

We now turn on the radiative decay rate associated with the 2D-LDOS in the interval $[-n_1k_0 : n_1k_0]$. We compare in Fig. 3(b) our numerical simulation with the quasistatic approximation derived in Refs. 5 and 24 for the nanowire. The quasistatic approximation underestimates the radiative contribution to the coupling rate since it only considers the cylindrical dipole mode.

Finally, the nonradiative decay rate γ_{NR} is determined from 2D-LDOS calculated on the evanescent domain $|k_z| > n_1k_0$ which includes all the nonradiative mechanisms: joule losses during plasmon propagation and electron-hole pair creation into the metal. Figure 3(c) represents the plasmon and total nonradiative rates. The nonradiative rate diverges close to the wire surface whereas the plasmon contribution remains finite. For large separation distances, the plasmon is the only contribution to the nonradiative rate. We achieve an optimal coupling efficiency into the guided SPP, $\beta = \gamma_{pl}/(\gamma_{rad} + \gamma_{NR}) = 83\%$, at $d = 20$ nm.

So far, we considered a silver circular nanowire embedded in a homogeneous background to illustrate and validate our method. In the following, we investigate the two complex geometries depicted in Figs. 1(b) and 1(c). Figure 4 presents the coupling rate into the SPP supported by a penta-twinned crystalline nanowire recently characterized.[25] At short distances, the coupling rate into the guided SPP is strongly enhanced as compared to coupling to a circular wire of similar dimensions. This is due to the strong mode confinement near the wire corners as revealed by the mode profile.

Experimental configurations generally concern structures deposited on a substrate. For a high-index substrate, the otherwise bound mode becomes leaky. Note that the usual expression (10) is then practically unenforceable due to difficulty of normalizing the mode. Differently, expression (9), derived in this work, is easily used even in such a situation. Moreover, in the case of a leaky mode, it is even more difficult to properly distinguish radiative and nonradiative contributions to the coupling rate, as compared to the bound mode situation treated above. Indeed, the guided plasmon contributes to both the radiative rate (leaky part) and nonradiative transfer (intrinsic losses). This difficulty is easily overcome using the
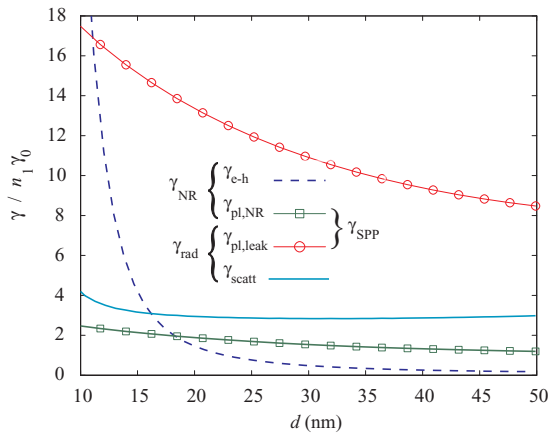
FIG. 5. (Color online) Different contributions to the decay rates for a 100 nm diameter silver wire 50 nm above a glass substrate ($\epsilon_3 = 2.25$). Superstrate is air ($\epsilon_1 = 1$).

2D-LDOS formalism. The propagation length can be written $L_{SPP} = (\Gamma_{rad}^{SPP} + \Gamma_{nrad}^{SPP})^{-1}$ where the radiative and nonradiative rates have been introduced. As an example, we consider a 100 nm silver nanowire 50 nm above a glass substrate [Fig. 1(c)]. We calculate an effective index $n_{eff} = 1.28$, below the substrate optical index, indicating a leaky mode. Its

propagation length is $L_{SPP} = 1.2$ μm $= 1/\Gamma^{SPP}$ with $\Gamma^{SPP} = 0.083$ μm^{-1}. The leakage rate is evaluated by canceling the metal losses [Im(ϵ_2) = 0]. We obtain $\Gamma_{rad}^{SPP} = 0.073$ μm^{-1}. Figure 5 shows the interplay between the various contributions to the decay rate for an emitter placed in the wire-substrate gap. The radiative rate $\gamma_{rad} = \gamma_{scatt} + \gamma_{pl,leak}$ is the sum of the scattering and leakage channels, and the nonradiative rate $\gamma_{NR} = \gamma_{pl,NR} + \gamma_{e-h}$ originates from plasmon losses and electron-hole pair creation. Except for short distances, the main decay channel is the plasmon decoupling into the substrate. We obtain a maximum decoupling emission into the substrate $\beta = \gamma_{pl,leak}/\gamma = 70\%$ for an emitter centered in the gap ($d = 25$ nm).[26]

To conclude, we derive an explicit expression for the coupling rate between a point-like quantum emitter and a 2D plasmonic waveguide. We define the coupling Purcell factor into the plasmon channel whereas the radiative and nonradiative rates are numerically investigated. This method clearly reveals the physics underlying the complex mechanisms of spontaneous emission coupled to a plasmonic guide (scattering, leakage, electron-hole pair creation, SPP excitation).

*gerard.colas-des-francs@u-bourgogne.fr

[1]E. Purcell, Phys. Rev. **69**, 681 (1946).

[2]K. Vahala, Nature (London) **424**, 839 (2003).

[3]I. Maksymov, M. Besbes, J. P. Hugonin, J. Yang, A. Beveratos, I. Sagnes, I. Robert-Philip, and P. Lalanne, Phys. Rev. Lett. **105**, 180502 (2010).

[4]J. J. Greffet, M. Laroche, and F. Marquier, Phys. Rev. Lett. **105**, 117701 (2010).

[5]D. E. Chang, A. S. Sorensen, P. R. Hemmer, and M. D. Lukin, Phys. Rev. Lett. **97**, 053002 (2006).

[6]A. Cuche et al., Nano Lett. **10**, 4566 (2010).

[7]J.-C. Weeber et al., Nano Lett. **7**, 1352 (2007); Y. Gonga and J. Vuckovic, Appl. Phys. Lett. **90**, 033113 (2007).

[8]D. Chang et al., Nature Phys. **3**, 807 (2007); D. Dzsotjan, A. S. Sorensen, M. Fleischhauer, Phys. Rev. B **82**, 075427 (2010); A. Gonzalez-Tudela, D. Martin-Cano, E. Moreno, L. Martin-Moreno, C. Tejedor, F. J. Garcia-Vidal, Phys. Rev. Lett. **106**, 020501 (2011).

[9]I. De Leon and P. Berini, Phys. Rev. B **78**, 161401 (2008).

[10]J. Grandidier et al., Nano Lett. **9**, 2935 (2009).

[11]G. Colas des Francs et al., Opt. Express **18**, 16327 (2010).

[12]V. Zuev et al., J. Chem. Phys. **122**, 214726 (2005).

[13]K. Tanaka et al., Appl. Phys. B **93**, 257 (2008).

[14]X. Chen et al., Nano Lett. **9**, 3756 (2009).

[15]N. Issa and R. Guckenberger, Opt. Express **15**, 12131 (2007).

[16]G. Colas des Francs et al., J. Chem. Phys. **117**, 4659 (2002); J. Hoogenboom et al., Nano Lett. **9**, 1189 (2009).

[17]G. Colas des Francs, C. Girard, J.-C. Weeber, C. Chicane, T. David, A. Dereux, and D. Peyrade, Phys. Rev. Lett. **86**, 4950 (2001).

[18]O. Martin et al., Phys. Rev. Lett. **82**, 315 (1999); A. Asatryan et al., Phys. Rev. E **63**, 046612 (2001).

[19]F. J. García de Abajo and M. Kociak, Phys. Rev. Lett. **100**, 106804 (2008).

[20]G. Colas des Francs, J. Grandidier, S. Massenot, A. Bouhelier, J.-C. Weeber, and A. Dereux, Phys. Rev. B **80**, 115419 (2009).

[21]W. Barnes, J. Mod. Opt. **45**, 661 (1998).

[22]F. Le Kien, S. Dutta Gupta, V. I. Balykin, and K. Hakuta Phys. Rev. A **72**, 032509 (2005).

[23]Y. Chen, T. R. Nielsen, N. Gregersen, P. Lodahl, and J. Mork, Phys. Rev. B **81**, 125431 (2010).

[24]V. V. Klimov and M. Ducloy, Phys. Rev. A **69**, 013812 (2004).

[25]M. Song et al., ACS Nano **5**, 5874 (2011).

[26]I. Mallek Zouari et al., Appl. Phys. Lett. **97**, 053109 (2010).